Scripta Materialia 199 (2021) 113864

Contents lists available at ScienceDirect

Scripta Materialia

journal homepage: www.elsevier.com/locate/scriptamat

Micro-luminescence measurement to evidence decomposition of persistent luminescent particles during the preparation of novel persistent luminescent tellurite glasses

M. Hasnat [a], V. Lahti [a], H. Byron [b,c], M. Lastusaari [b,d], L. Petit [a,*]

[a] Photonics Laboratory, Tampere University, FI, 33101, Tampere, Finland
[b] University of Turku, Department of Chemistry, FI, 20014 Turku, Finland
[c] University of Turku Graduate School (UTUGS), Doctoral Programme in Physical and Chemical Sciences, FI, 20014, Turku, Finland
[d] Turku University Centre for Materials and Surfaces (MatSurf), Turku, Finland

ARTICLE INFO

Article history:
Received 14 December 2020
Accepted 7 March 2021
Available online 18 March 2021

ABSTRACT

The preparation of tellurite glasses with persistent luminescence by adding persistent luminescent particles in the glass melt is reported. Compared to phosphate glasses, the afterglow from the tellurite glasses is low, indicating that the tellurite melt is more corrosive on the particles than the phosphate melt. However, as opposed to phosphate glasses, no emission from Eu^{3+} was detected in the photoluminescence spectra of the glasses when crushed into powder. We show that a confocal Raman microscope can be used to evidence the presence of Eu^{3+} in the glass-particles interface confirming that some oxidation of Eu^{2+} actually takes place during the preparation of the tellurite glasses.

Persistent luminescent (PeL) materials have been of great interest for the past few decades, as these materials can find applications as safety signage, for example [1, 2]. Persistent luminescence (PeL), also called phosphorescence or afterglow, is defined as an emission which continues after the removal of the irradiation source [3]. The $SrAl_2O_4$:Eu,Dy luminophore is known as the most efficient luminescent persistent emitter, with strong and long (up to 20 hours) afterglow after ceasing the excitation [4]. This material has found uses in many applications such as emergency signs, in-vivo imagining, and luminescent coatings, to cite just a few examples [5,6].

The first PeL glass-ceramic was successfully prepared using the "frozen sorbet" method [7]. In this method, a heat treatment of a glass in the SrO-Al_2O_3-B_2O_3 system was used to precipitate the $SrAl_2O_4$:Eu^{2+},Dy^{3+} crystals. Since this promising PeL glass-ceramic, a great effort has been made on the preparation of glasses in other glass systems with persistent luminescence. Phosphate and borosilicate glasses were successfully prepared with persistent luminescence using the direct doping method [8,9]. In this direct doping method, the PeL particles are added directly in the glass melt [10].

In order to ensure the survival and dispersion of the PeL particles in the glass melt, the PeL particles should be added at a lower temperature than the melting temperature. As explained in [11], partial dissolution of the PeL particles in the glass matrix always occurs during the glass preparation due to the corrosive behavior of the glass melt, leading to a decrease in intensity of the afterglow from the glass. A scanning electron microscope (SEM) is usually used to evidence the dissolution of the PeL particles in the glass matrix which is associated with the diffusion of the elements of the particles into the glass. The partial dissolution of the PeL particles then leads to the oxidation of some Eu^{2+} to Eu^{3+} in the glass, causing the appearance of emission lines between 575 and 650 nm in the conventional emission spectrum of the glass. Therefore, it is crucial to optimize the direct doping parameters, such as the temperature at which the PeL particles are added in the glass melt, to limit the decomposition of the particles in the glass. Furthermore, a recent study showed that the composition of the glass melt has a significant impact on the decomposition of the particles [9], clearly showing the need to investigate further the impact of other glass melts on the corrosion of PeL particles during the glass preparation.

Here, the preparation of new PeL glasses with larger optical basicity than phosphate glasses and the characterization of their spectroscopic properties are reported. The glasses of investigation

* Corresponding author.
E-mail address: laeticia.petit@tuni.fi (L. Petit).

https://doi.org/10.1016/j.scriptamat.2021.113864

are tellurite glasses with the composition $70TeO_2$-$10Bi_2O_3$-20ZnO (in mol %). The impact of the tellurite glass melt on the corrosion of PeL particles is discussed.

The glasses were prepared using TeO_2 (Sigma Aldrich, 99%), Bi_2O_3 (Sigma Aldrich, 99.99%) and ZnO (Sigma-Aldrich, ≥99.5%). The glasses were melted in a Pt crucible at 850 °C for 5 min. The temperature was then reduced to the doping temperature (T_{doping}) prior to adding 1 wt % of commercial $SrAl_2O_4:Eu^{2+},Dy^{3+}$ microparticles (MPs) (Jinan G.L. New Materials, China, YG - 101). The doping temperatures were between 550 and 650 °C (glasses are labeled Te550, Te575, Te600, Te625 and Te650, respectively). The glasses were cast 3 min after adding the MPs and annealed for 4 hours at 250°C to remove residual stresses from the quench.

Phosphate glasses (Phos) with the composition $50P_2O5$-$10Na_2O$-40SrO (mol%) were prepared with the same amount of PeL particles and with different T_{doping} ranging from 975 to 1025 °C (glasses are labeled Phos975, Phos1000 and Phos1025). The details of the PeL phosphate glass preparation as well as the spectroscopic properties of these glasses can be found in [11].

The photoluminescence (PL) spectra of the PeL glasses (λ_{exc}: 266 nm, Nd:YAG pulse laser, 8 ns, TII Lotis) were measured using a CCD camera (Avantes, AvaSpec HS-TEC). The persistent luminescence (PeL) spectra of the PeL glasses were measured at room temperature using a Varian Cary Eclipse Fluorescence Spectrophotometer equipped with a Hamamatsu R928 photomultiplier (PMT). For the PeL measurements, the samples were irradiated for 5 min at room temperature with a compact UV lamp (UVGL-25, 4 W, λ_{exc}: 254 nm) and the PeL spectra were collected 1 min after stopping the irradiation.

For the PeL fading measurements, the samples were irradiated for 5 min with a 254 nm hand-held UV-lamp (UVGL-25). The luminance fading curves were obtained by measuring the luminance every 1 s starting 1 min after stopping the excitation using a Hagner ERP-105 luminance meter. The time taken for PeL luminance to decay down to 0.3 mcd/m^2 is referred to as the PeL decay time. The accuracy of the decay time was determined from the noise level of each individual measurement- It ranged from ±0.2 to 5 min (see the error bars in Fig. 1). The PeL lifetimes were obtained with two-component exponential decay fitting of the luminance fading curves using OriginLab Origin software. The two components of the fitted decay curves were weighted with their amplitudes to obtain the average lifetime, i.e. the time needed for the intensity to drop to 1/e of the initial intensity. The accuracy of the average lifetime was obtained from exponential decay fits. It ranged from ±0.03 to 0.24 min (see the error bars in Fig. 1).

A scanning electron microscope (Carl Zeiss Crossbeam 540) equipped with Oxford Instruments X-Max^N 80 EDS detector was used to image the PeL particles in the glass and to analyze the composition of the samples. The accuracy of the elemental analysis was ± 1.5 mol%.

The micro-luminescence spectra were recorded using an inVia Qontor confocal Raman microscope (Renishaw, Gloucestershire, UK). The emission spectra were recorded using 405 and 532 nm CW laser excitations to detect Eu^{2+} and Eu^{3+} emission respectively.

Persistent luminescent particles with the $SrAl_2O_4:Eu^{2+},Dy^{3+}$ composition were added in tellurite (Te) glass ($70TeO_2$-$10Bi_2O_3$-20ZnO (in mol %)) at temperatures ranging from 550 to 650°C. The chosen doping temperature (T_{doping}) is lower than the melt-

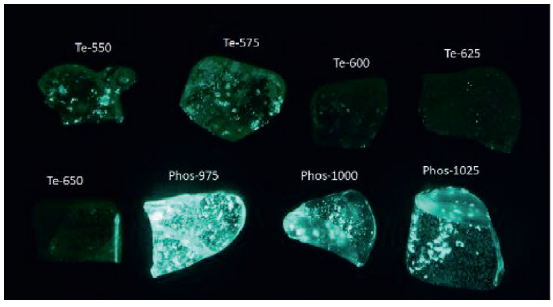

c)

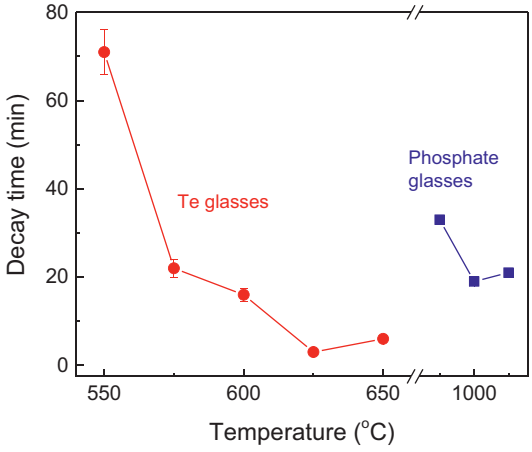

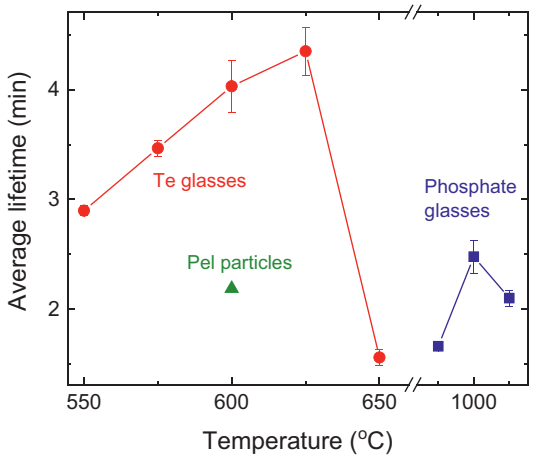

Fig. 1. Afterglow picture of the tellurite (Te) and phosphate (P) glasses prepared using different doping temperatures (a). The picture was taken after stopping the 254nm irradiation. Average PeL lifetimes obtained with exponential fitting (b). PeL decay times down to 0.3 mcd/m^2 (c). Note: in some cases, the estimated standard deviations (esd) are smaller than the symbol sizes.

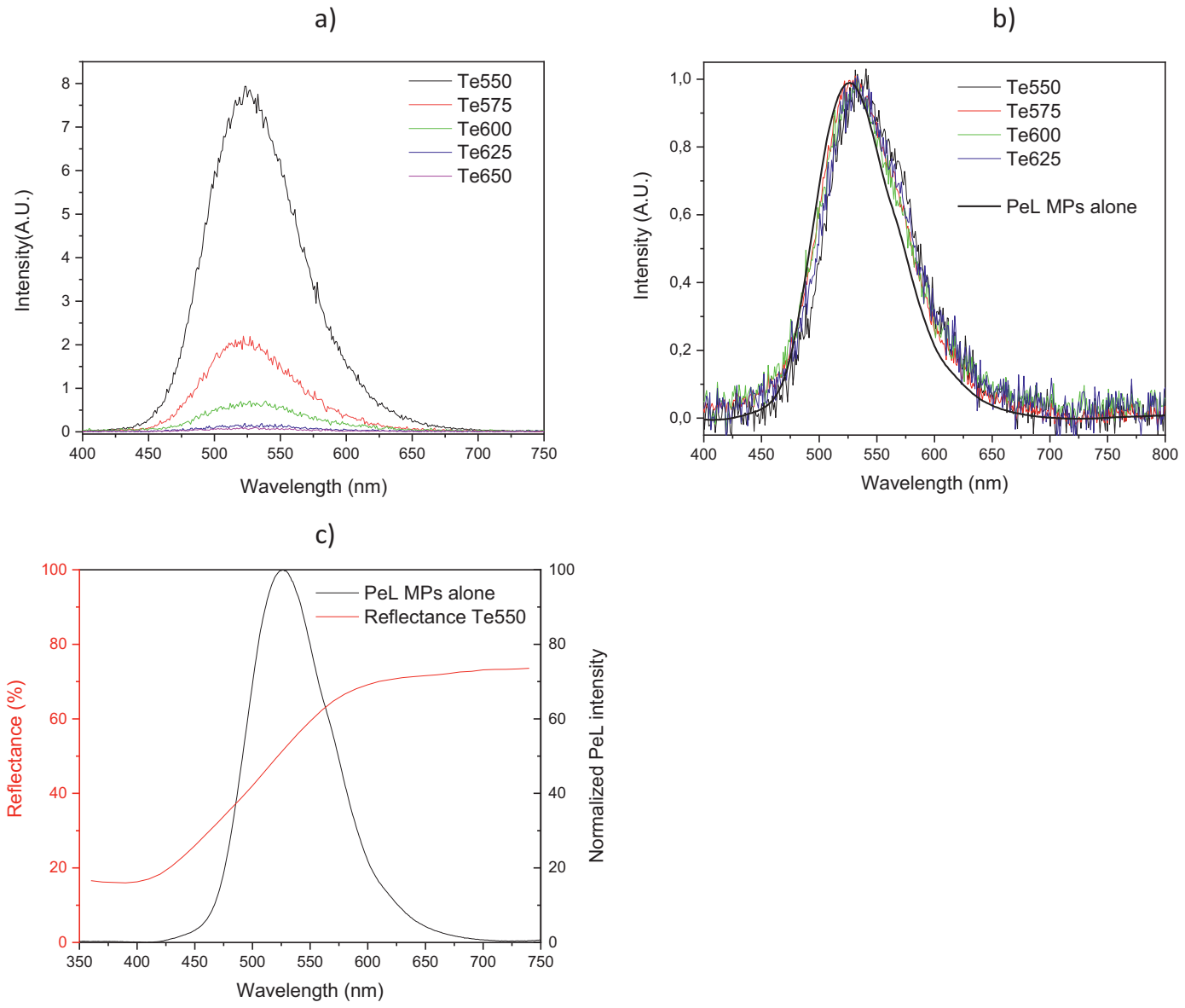

Fig. 2. Persistent luminescence (PeL) (a) and normalized photoluminescence (PL) (b) spectra of the investigated glasses. Reflectance spectrum of the Te550 glass, taken as an example, and the PeL emission spectrum of the microparticles (MPs) alone (c).

ing temperature to ensure the survival of the particles but remains high enough so the glass melt is viscous enough to ensure the dispersion of the particles in the glass. As explained in [8,9,11], the survival of the particles during the glass preparation is confirmed from the afterglow of the glasses. PeL could be seen from the Te glasses prepared using T_{doping} lower than 600 °C, whereas no PeL was visible to the eye from the Te625 and Te650 glasses (Fig. 1a). The PeL is not as uniformly distributed as desired, because of the presence of PeL particle agglomerates in the glasses. Also shown in Fig. 1a is the afterglow picture of phosphate (Phos) glasses with the composition $50P_2O_5$-$10Na_2O$-40SrO (mol%), prepared with the same amount of PeL particles and with different T_{doping}. When compared to the Phos glasses, the initial afterglow of the Te glasses is less bright despite the use of lower T_{doping}. As explained in [8,9,11], a decrease in the intensity of the PeL can be related to the corrosion of the PeL particles by the glass melt occurring during the glass preparation. Thus, the Te glass melt is expected to be more corrosive to the particles than the Phos glass melt.

The average PeL lifetime of the Te and P glasses, in Fig. 1b, shows that the PeL fading of the Te glasses is a significantly slower process compared to that of Phos glasses. Fig. 1c presents the decay time for each glass, i.e. the length of time PeL is visible to the human eye after excitation has ceased. For both the Te and the Phos glasses, the increase in the T_{doping} shortens the duration that PeL remains visible. These observations can be explained by considering two different effects the particles undergo when embedded in the glass matrix. The first effect is the corrosion of the PeL particles by the glass matrices and concerns the size of the particles present in the glasses and therefore the number of traps present. The decrease in the PeL decay time with an increase in T_{doping} for both glass systems seen in Fig. 1c indicates that an increase in T_{doping} lowers the trap density for storing and releasing the energy as PeL. The second effect concerns the structure of the traps themselves and how they change when the particles are embedded in the glass matrix. It seems that in the Phos glasses, the average PeL lifetime is practically the same as it is for the bare PeL particles, but in the Te glasses it is clearly longer (Fig. 1b). Since

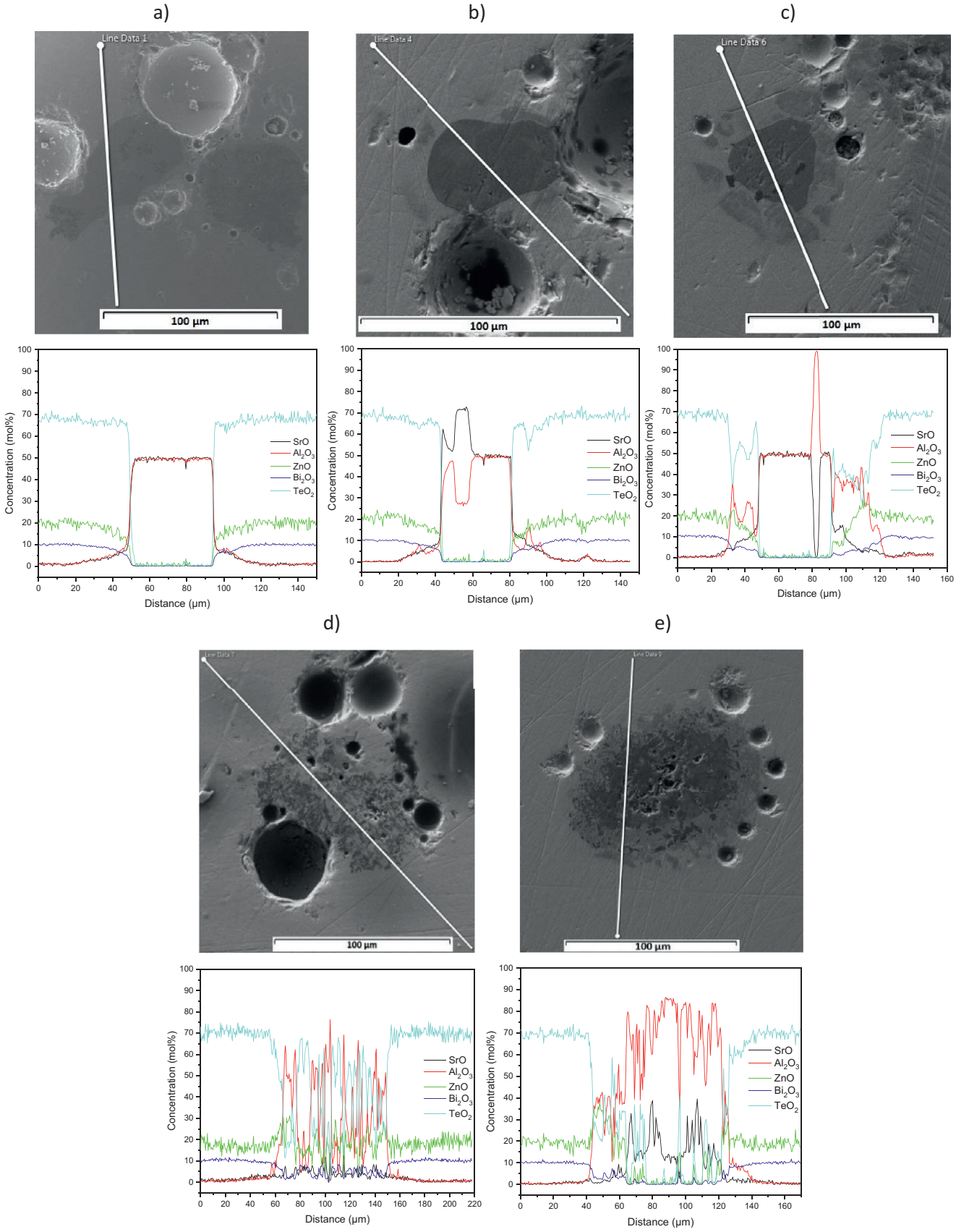

Fig. 3. SEM/Composition analysis across a PeL particle found at the surface of each of the PeL glasses prepared using different doping temperatures: 550 °C (a), 575 °C (b), 600 °C (c), 625 °C (d) and 650 °C (e).

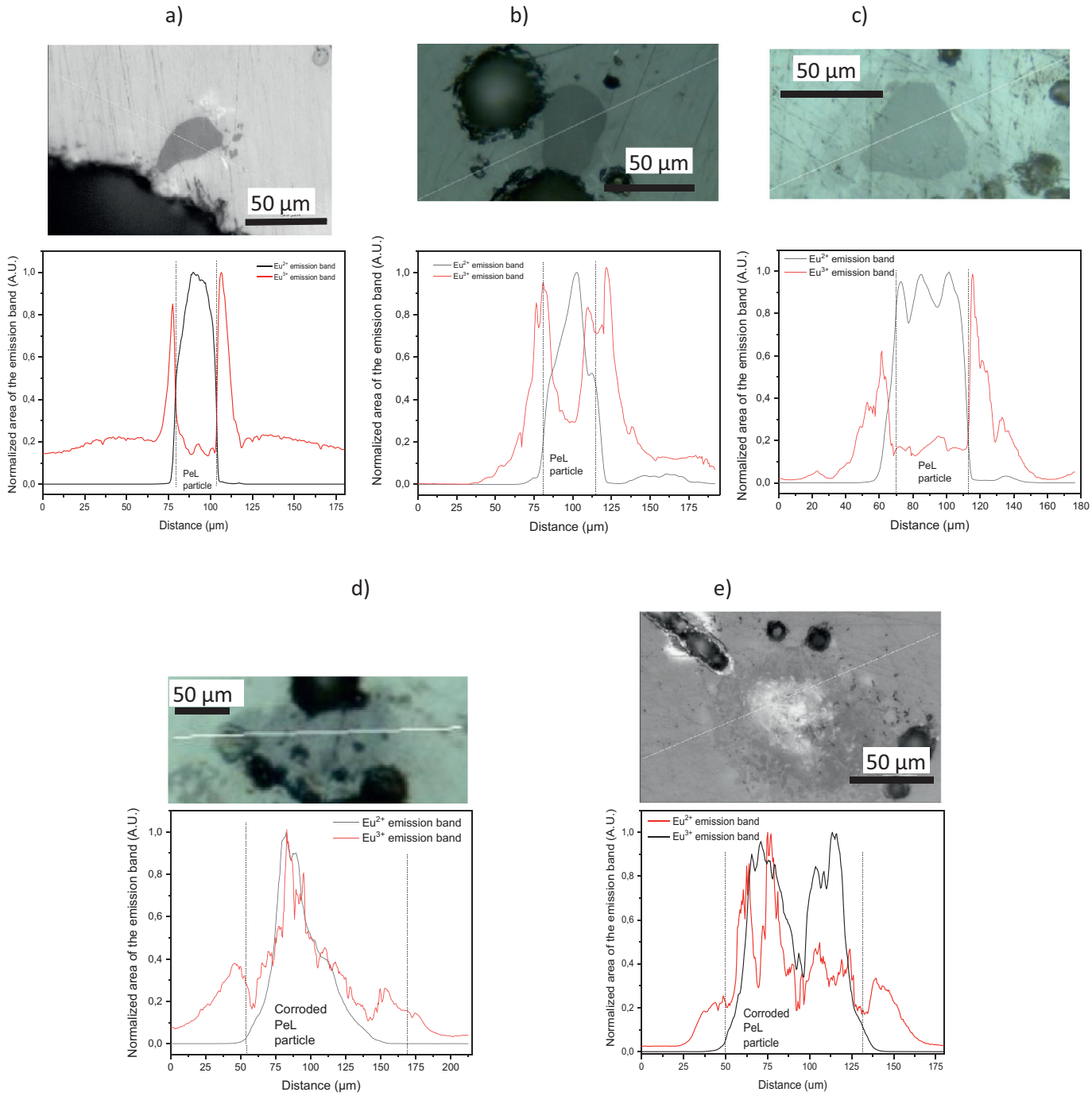

Fig. 4. Profile of the normalized area of the Eu^{2+} and Eu^{3+} emission bands across a PeL particle found at the surface of each of the PeL glass prepared using different doping temperatures: 550 °C (a), 575 °C (b), 600 °C (c), 625 °C (d) and 650 °C (e).

the PeL decay process, which corresponds to the emptying of the electron traps, can be thought of as following the Boltzmann distribution, the increase in the average PeL lifetime indicates either an increase in the number of electron traps or a deepening of the traps. If we consider the fact that the Te550 glass shows longer PeL visible to the eye than the Phos glasses (Fig. 1c) despite its lower trap density due to corrosion by the Te glass melt, it is more probable that the deepening of the traps would be the dominant effect to explain the long average PeL lifetime of the Te glasses. This is thought to be the result of a chemical effect of the Te glass melt on the PeL particles. However the mechanism causing the deepening is beyond the scope of this report. As a result of the deepening of the traps and of the comparatively little corrosion of the PeL particles at T_{doping} = 550°C, the afterglow from the Te550 glass stays visible to the naked eye longer than that from any of the Phos glasses (Fig. 1c). With increasing T_{doping}, the PeL decay time of the Te glasses decreases, finally ending up below those for the Phos glasses. From this, it is thought that as the T_{doping} rises, the trap density is reduced and thus, the corrosion effect is dominant over the trap deepening in the Te glass matrix. A similar, albeit weaker trend is observed for the Phos glasses.

The PeL spectra of the glasses, depicted in Fig. 2a, exhibit a broad band centered at 523 nm which is due to the $4f^6 5d^1 \rightarrow 4f^7$ transition in Eu^{2+} located in one site in the monoclinic $SrAl_2O_4$

structure [12]. In agreement with Fig. 1a, the intensity of the PeL emission, recorded 1 min after stopping excitation, decreases as the T_{doping} increases. Similar decrease in the intensity of the PeL was reported when preparing PeL phosphate and borosilicate glasses with an increase in the T_{doping} and is a clear sign of the progressive decomposition of the particles as T_{doping} increases [8,9,11]. The PeL decay time after 254 nm charging, which usually lasts about 35 h for free MPs, decreases after being embedded in the glasses; it further decreases from 70 to ~10 min in Te glasses when the T_{doping} increases from 550 to 650°C, confirming the decomposition of the PeL particles occurring during the preparation of the Te glasses (Fig. 1c). Nonetheless, as shown in Fig. 2c, the local structure of the Eu^{2+} is not impacted after embedding the PeL particles in the glasses. Indeed, the conventional luminescence spectra of the glasses exhibit a broad band confirming that Eu^{2+} ions are located in one site in the monoclinic $SrAl_2O_4$ structure. One can notice that the position of the emission band is slightly shifted to a longer wavelength after embedding the PeL particles in the glasses. As previously reported in [8,9,11], a shift of the emission band can be related to changes in the site of Eu^{2+} induced by the partial decomposition of the PeL particles during the glass preparation. However, because the Te glasses possess a yellowish body color, the apparent PeL color is affected by the absorption of the glass matrix as shown in Fig. 2c which also presents the reflectance spectrum of the Te550 glass, taken as an example, and the PeL spectrum of the bare PeL MPs. One should mention that all glasses exhibit similar reflectance spectra.

The decomposition of the PeL particles occurring during the glass preparation was evidenced using SEM coupled with EDS analysis. As shown in Fig. 3, the morphology and the composition of the PeL particles change as the T_{doping} increases: completely corroded/decomposed PeL particles were seen at the surface of the Te625 and Te650 glasses, which is in agreement with the absence of afterglow from these glasses. Yet, the PeL particles maintain their composition in their center in the Te550 and Te575 glasses, which is in agreement with the afterglow observed from these glasses. One can also notice the presence of Al and Sr in the glass at the glass – PeL particle interface confirming the decomposition of the PeL particles, associated with the diffusion of Al and Sr into the glass. One should point out that the decomposition of the PeL particles already occurs at 550°C even though the glass prepared at this T_{doping} exhibits PeL. The diffusion distance of Al and Sr is suspected to be ~20-30 µm around the particles found in the Te550 and Te575 glasses.

Surprisingly, compared to our previous studies [8,9,11], no emission lines at 590, 610 and 680 nm were seen in the PL spectra presented in Fig. 2b, although these lines could be observed in the PL spectra of phosphate and borosilicate glasses [8,9,11]. One should be reminded that these lines are typical of emission from Eu^{3+} due to oxidation of some Eu^{2+} ions to Eu^{3+} ions occurring during the glass melting. The absence of Eu^{3+} emission from the Te glasses when crushed into powder, despite the obvious decomposition of the PeL particles occurring during the glass melting, might be related to the high optical basicity of the tellurite glasses compared to that of the phosphate glasses. The theoretical optical basicity of the glasses was determined as in [13,14]:

$$\hat{}th = \chi_1\hat{}_1 + \chi_2\hat{}_2 + \ldots + \chi_n\hat{}_n \quad (1)$$

where χ_1, χ_2,... χ_n represent the equivalent fractions of each oxide which contribute to the overall material stoichiometry and $\hat{}_1$, $\hat{}_2$... $\hat{}_n$ stands for the optical basicity of each individual oxide in the glass system. The optical basicity of each oxide is $\hat{}(TeO_2) = 0.95$, $\hat{}(Bi_2O_3) = 1.19$, $\hat{}(ZnO) = 1.03$, $\hat{}(Na_2O) = 1.15$, $\hat{}(P_2O_5) = 0.33$ and $\hat{}(SrO)=1.08$ [15,16].

The theoretical optical basicity of the phosphate and tellurite glasses is estimated at 0.457 and 0.996, respectively. It is probably due to the high optical basicity of the tellurite glass compared to phosphate glass that less oxidation of Eu^{2+} is expected to occur during the preparation of the PeL tellurite glass.

Nonetheless, the presence of Eu^{3+} in the tellurite glasses was confirmed using a confocal Raman microscope which allowed the measurement of the emission spectra at the glass-PeL particles interface. The emission spectra were recorded using different excitation wavelengths in order to measure the emission from Eu^{2+} and Eu^{3+}. Under 405 nm excitation, the glasses exhibit an emission band centered at 495 nm which could be attributed to the Eu^{2+} d-f transitions, while an emission centered at 612 nm due to the $^5D_0 \rightarrow {}^7F_2$ transitions of Eu^{3+} [17] was observed after 532nm excitation. For all the investigated glasses, both emissions could be detected, confirming that the oxidationof Eu^{2+} also occurs in tellurite glasses during the glass preparation. The area of the emission bands at 495 and 612nm were normalized to the maximum and plotted as a function of the distance from the particles to the glass. Fig. 4 depicts the relative changes in the area of the Eu^{2+} and Eu^{3+} emission bands measured across a PeL particle found at the surface of the investigated glasses. Particles with a size of ~40 µm were found at the surface the Te550, Te575 and Te600 glasses exhibiting Eu^{2+} emission. At the glass-particle interface, emission from Eu^{3+} could be detected at the expense of the emission from Eu^{2+} confirming that as for Al and Sr, Eu^{2+} ions also diffuse inside the glass (~40 µm from the particles) during the glass preparation and oxidize to Eu^{3+}. However, as compared to phosphate glasses, a lower amount of Eu^{2+} ions is expected to oxidize in the tellurite glasses as no Eu^{3+} emission could be detected in the PL spectra measured using crushed glasses. As observed with the SEM, the particles in the Te625 and Te650 look corroded but they still exhibit some emission from Eu^{2+}.

In summary, new tellurite glasses with PeL were successfully prepared by adding PeL particles in the glass melt using the direct doping method. However, compared to phosphate glasses, the initial intensity of the afterglow from the tellurite glass is small, confirming the strong corrosive behavior of the tellurite glass melt on the PeL particles. On the other hand, the PeL decay time of the tellurite glass prepared using a T_{doping} of 550°C is much slower than that of the phosphate glasses probably due to traps in the PeL particles becoming deeper in this glass. As opposed to phosphate glasses, no emission from Eu^{3+} could be seen in the PL spectra of the tellurite glasses when crushed into powder, but it could be detected around the PeL particles using a confocal Raman microscope. This confirms that the oxidation process of Eu^{2+} to Eu^{3+} also takes place during the preparation of the tellurite glasses, but this process is less than in phosphate glass, probably due to the high optical basicity of the tellurite glass.

Declaration of Competing Interest

The authors declare that they have no known competing financial interests or personal relationships that could have appeared to influence the work reported in this paper.

Acknowledgements

Academy of Finland (Flagship Programme, Photonics Research and Innovation PREIN-320165 and Academy Project -326418) is greatly acknowledged for the financial support. Dr. Veber is also acknowledged for fruitful discussion.

References

[1] C. Chang, Z. Yuan, D. Mao, J. Alloys Compd. 415 (2006) 220–224.
[2] Y. Li, M. Gecevicius, Chem. Soc. Rev. 45 (2016) 2090.
[3] T. Aitasalo, J. Hölsä, H. Jungner, M. Lastusaari, J. Niittykoski, J. Phys. Chem. *B* 110 (2006) 4589–4598.

[4] T. Matsuzawa, Y. Aoki, N. Takeuchi, Y. Murayama, Journal of The Electrochemical Society, 143(8) (10̸996) 2670–2673.
[5] K. Van den Eeckhout, P.F. Smet, D. Poelman, Mater. 3 (2010) 2536–2566.
[6] Q. Le Masne de Chermont, C. Chaneac, J. Seguin, F. Pelle, S. Maîtrejean, J.-P. Jolivet, D. Gourier, M. Bessodes, D. Scherman, Proceedings of the National Academy of Sciences 104 (22) (2007) 9266–9271.
[7] T. Nakanishi, Y. Katayama, J. Ueda, T. Honma, S. Tanabe, T. Komatsu, J. Ceram. Soc. Jpn. 119 (2011) 609–615.
[8] P. Roldán Del Cerro, T. Salminen, M. Lastusaari, L. Petit, Scripta Materialia 151 (2018) 38–41.
[9] N. Ojha, T. Laihinen, T. Salminen, M. Lastusaari, L. Petit, Ceramics International 44 (2018) 11807–11811.
[10] J. Zhao, X. Zheng, E.P. Schartner, P. Ionescu, R. Zhang, T-L. Nguyen, D. Jin, H. Ebendorff-Heidepriem, Adv. Optical Mater. (2016), doi:10.1002/adom.201600296.
[11] N. Ojha, H. Nguyen, T. Laihinen, T. Salminen, M. Lastusaari, L. Petit, Corrosion Science 135 (2018) 207–214.
[12] H. Yamamoto, T. Matsuzawa, J. Lumin, 72-74 (1997) 287-289.
[13] J.A. Duffy, B. Harris, E.I. Kamitsos, G.D. Chryssikos, Y.D. Yiannopoulos, J. Phys. Chem. B 101 (1997) 4188–4192.
[14] J.A. Duffy, Geochim. Cosmochim. Acta 57 (1993) 3961–3970.
[15] T. Honma, Y. Benino, T. Fujiwara, T. Komatsu, R. Sato, V. Dimitrov, J Appl Phys 91 (2002) 2942–2950.
[16] L.L. Velli, C.P.E. Varsamis, E.I. Kamitsos, D. Möncke, D. Ehrt, Phys Chem Glasses-Eur J Glass Sci Technol Part B 49 (2008) 182–187.
[17] F. Zhang, S. Chen, J.F. Chen, H.L. Zhang, J. Li, X.J. Liu, S.W. Wang, Journal of Applied Physics 111 (2012) 083532.